NONLINEAR AND LOGISTIC GROWTH IN EXPERIMENTAL POPULATIONS OF GUPPIES[1]

JAY BARLOW
*Southwest Fisheries Science Center, National Marine Fisheries Service, P.O. Box 271,
La Jolla, California 92038 USA*

Abstract. Previous experiments have shown that for a specific experimental system of guppies (*Poecilia reticulata*), per capita growth rate is linearly related to population biomass. A length-specific population model is developed to examine how the various mechanisms of density dependence (i.e., changes in somatic growth rates, reproductive rates, and cannibalism) act in concert to shape the overall population response to intraspecific competition. Despite many nonlinear components, equilibrium per capita growth in the model is linearly related to population biomass, mimicking the logistic growth seen in the experiment. Using the model, the components of density dependence are varied to determine how each component shapes the overall density-dependent response. Density dependence in somatic growth rates is found to be the most important population-regulating mechanism in this system. In the past, emphasis has been placed on density dependence in birth and death functions. The importance of somatic growth in shaping per capita population growth curves may be underestimated.

Key words: density dependence; guppy; intraspecific competition; logistic; nonlinear dynamics; per capita growth rate; Poecilia; *population dynamics.*

INTRODUCTION

Logistic growth refers to a particular form of density dependence in which per capita growth rate declines linearly with population size. In the early 1900s, Raymond Pearl attempted to convince a skeptical world that the logistic represented a universal law of population growth (Kingsland 1985). Subsequent studies have shown that density dependence often differs significantly from the simple, linear predictions of the logistic. Differences from the logistic are believed to be important in promoting stability between competing species of *Drosophila* in experimental systems (Gilpin and Ayala 1973, Pomerantz et al. 1980). Furthermore, evidence is accumulating that species with particular life histories, such as long-lived mammals (Fowler 1981, 1988) or species that feed higher on a food chain (May et al. 1979), deviate from the logistic growth model in a consistent, predictable manner. This is strengthened by analyses that suggest that the form of density dependence can, itself, be subject to natural selection (Gilpin et al. 1976, Gill 1978). Nonlogistic growth curves are currently being used in the management of marine mammals (Smith 1983) and other species.

For nonlogistic density dependence (e.g., the θ-logistic model of Gilpin et al. 1976), per capita growth rate is typically modeled as a nonlinear function of population size (measured in numbers of individuals or population mass). Such models suffice as empirical representations of density dependence but give little

insight into the factors that shape population growth. Increasing population size can affect somatic growth rates, survival rates, birth rates, age at maturation, etc. I will refer to these effects as the mechanisms of density dependence. The functional relationship between per capita growth rate and population density is likely to depend on which of these mechanisms function to limit population growth. For instance, Goodman (1980) showed that when the density-compensating mechanism was a linear relationship between fecundity and population size, the resulting per capita growth rate is a concave (θ > 1 in the θ-logistic model), nonlinear function of population size. Kerfoot et al. (1985) showed the converse, that certain nonlinear mechanisms can result in a linear relationship between per capita growth rate and population size.

In this paper I investigate how population growth curves are shaped by various mechanisms of density dependence. I limit my investigations to actual mechanisms that were measured in an experimental system that shows logistic growth (Barlow 1982). In this system, guppy (*Poecilia reticulata*) populations experience growth limitation due to resource competition and cannibalism. Somatic growth, reproduction, and juvenile mortality were measured at a variety of different tank densities. Populations were forced to grow at constant per capita growth rates by maintaining constant per capita harvest rates (following the Smith-Gause culture dilution approach, Smith 1963). Models are fit to describe changes in these traits as continuous functions of population size. These submodels of density dependence for particular mechanisms are incorporated into an overall model that describes the dynamics of the

populations. By changing the various submodels of density-dependent mechanisms, I determine how each of these mechanisms act in shaping overall population growth as a function of population size.

METHODS

Experimental design

Fifteen experimental populations were established in 39-L glass aquaria. Each was fed a combination of dried flake food (0.21 g dry mass Tetra Min Staple Food) and frozen *Daphnia* (0.05 g dry mass) 6 times per week. Populations were harvested at 2-wk intervals. Harvests were taken as a constant percentage of the population size and were applied randomly over all size classes. Five harvest rates were used (5, 10, 15, 20, and 25% biweekly) with three replicates at each rate. Populations were allowed to grow for a total of 36 harvest periods (72 wk) under constant conditions. Populations approached stable size-frequency distributions while growing at a constant rate (determined by the harvest rate). During the course of the experiment, information was collected on length–frequency distributions within each population, somatic growth rates, individual fecundity rates, and population sex ratios.

Brackish water was circulated continuously between the five tanks within each of the three replicates. Water was also passed through external filter boxes using gravel as a filter medium. Thermostatically controlled heaters within the filter boxes maintained tank temperature between 23° and 25°C. Half of the water in each tank was discarded every 2 wk, and the remainder was passed through a combination of a diatom and activated carbon filter and an ultraviolet sterilizer. The discarded water was replaced with a brackish mixture of 50% seawater and 50% deionized water. Overhead fluorescent lights provided a 14:10 L:D diel cycle. The entire experimental system was housed in a plywood enclosure, isolating it from changes in ambient light and temperature.

Several structures were placed within the tanks to reduce juvenile mortality due to cannibalism. Previous experiments with guppies have shown that uncontrolled cannibalism leads to cyclic populations (Breder and Coates 1932, Shoemaker 1944, Laakso 1959). Following the design of Silliman and Gutsell (1958), 10 cm wide fences were constructed from 3 mm vertical glass rods spaced 1.5 mm apart. This fence was placed diagonally across one corner of each tank to provide an absolute refuge for small fish. Very few young survived during preliminary experiments with this system, therefore additional structure was added. Eight plastic mesh baskets (1-pint [55 mL] grocery berry baskets) were placed in each tank. Juvenile survival then increased to acceptable levels. The only other structures within the tanks were the water pump intakes and siphons, which equilibrated water level between tanks; both were screened to prevent movement of fish into the filter or between tanks.

The harvesting procedure consisted of removing a percentage of the fish present in each tank at biweekly intervals. Prior to harvests, fish were immobilized with MS-222 (ethyl-m-aminobenzoate) to facilitate handling. Population size was determined, and harvested fish were chosen randomly with respect to sex and size. Randomization and selection procedures are described by Barlow (1982). During alternate harvests (i.e., at 4-wk intervals), 35mm photographs were taken of the anesthetized fish in each population for later measurement of the length of each individual. Harvested fish were preserved in ethanol and were later used to determine length distributions, fecundity rates, and length/mass relationships. For the latter, 206 harvested fish were measured, dried, and weighed. Mass was determined to the nearest 1 mg after drying in an oven at 60°C for a minimum of 6 h.

Model design

A sex- and length-specific population projection model is formulated to describe the dynamics of the experimental system. Given initial length–frequency vectors for males and females, the model calculates the expected length–frequency vectors after one time period. The projection accounts for somatic growth (changes in length), births, adult mortality (harvest), and juvenile mortality (harvest and cannibalism). The model is purely deterministic and allows fractional representation in a length class.

Somatic growth is modeled with the Von Bertalanffy growth function. Length, L, is expressed as a function of initial length (L_i), time (t), and two parameters:

$$L(L_i, t) = L_\infty - [(L_\infty - L_i) \cdot \mathrm{Exp}(-k \cdot t)]. \quad (1)$$

The parameter L_∞ represents the asymptotic length, and k determines the rate at which length approaches that asymptote. The above equation is fit separately for males and females.

In the model, individuals are assigned to 1 mm length classes. To determine the growth of individuals within a length class, the expected lengths after one time interval are projected using both the minimum and maximum lengths of that length class as L_i in Eq. 1. Individuals are assigned to new length classes based on the assumption that they are uniformly distributed between the projected minima and maxima. As an example, if the 22–23 mm length class contains only one fish and if the expected lengths after one time period are 22.5 and 24.0 mm (for 22.0 and 23.0 mm fish, respectively), the single fish would be distributed as 1/3 in the 22–23 mm length class and 2/3 in the 23–24 mm length class.

As in the above example, not all the fish within a length class will necessarily enter another length class. In this case, a fraction of individuals remain in that length class indefinitely (although this fraction declines

exponentially with time). This is analogous to having nonzero elements on the principal diagonal of a population projection matrix. The effect can be minimized by having a large number of small length classes. There are, however, some desirable characteristics of having large length classes. If a group of fish of a given size is allowed to grow using the above algorithm, their size distribution would widen, thus mimicking the sort of natural variability in growth that would be expected in real populations. Length classes of 1 mm were found to be appropriate to mimic the level of individual variability seen in guppy growth (Barlow 1982).

The birth rate for mature females is modeled as a product of brood size and the rate of brood production. The birth rate, b, of a mature female of length L is thus given by:

$$b(L) = r \cdot F(L), \tag{2}$$

where r is the rate of brood production, and $F(L)$ is the brood size as a function of length. Brood size is modeled as a power function of length:

$$F(L) = \gamma \cdot L^\epsilon, \tag{3}$$

where γ and ϵ are parameters that shape the relationship between brood size and length. Females are assumed to mature at a specific length (i.e., knife-edge maturation). In the projection model, all individuals within a length class are assigned the birth rate corresponding to the midpoint of that interval. Births are distributed equally as males and females. Births are assumed to occur uniformly during the 2-wk time step of the model. Earlier births are discounted by juvenile mortality rate. Surviving young are assigned to length classes based on the assumption that they are uniformly distributed in size between the size at birth (6.5 mm) and the projected size at 2 wk (from Eq. 1).

Harvests contribute to juvenile mortality and are assumed to be the only source of adult mortality. In the model, this source of mortality is applied by multiplying the number of individuals in each length class by the escapement rate (i.e., the complement of the harvest rate).

Juvenile mortality was largely due to cannibalism. Based on observations made during the course of the experiment, the risk of mortality due to cannibalism decreases rapidly with size (Barlow 1982). Juvenile mortality is therefore modelled as an exponentially decreasing function of length. Insufficient information was gathered to estimate the rate at which cannibalism decreased with length. I assume that the risk of mortality due to cannibalism decreases by 50% with each millimetre of growth. The instantaneous rate of mortality due to cannibalism, $\mu(L)$, is thus given by:

$$\mu(L) = \mu_0 \cdot 0.5^{(L-L_0)}, \tag{4}$$

where μ_0 is the initial risk of mortality at birth, and L_0 is the size at birth. The survival rate, $s(L)$, is the complement of the death rate, $d(L)$, and represents the fraction of juveniles in a given size class that would survive one time step:

$$s(L) = 1 - d(L) = e^{-\mu(L)}, \tag{5}$$

where length, L, is taken as the midpoint of the length class.

Total tank biomass, M, is used as the measure of population density. Tank biomass is estimated by applying a length/mass relationship to the length–frequency vector. Individual mass, m, is assumed to be a power function of length:

$$m(L) = \alpha \cdot L^\beta. \tag{6}$$

Separate length/mass relationships are used for juveniles (<12 mm), males (>12 mm), and females (>12 mm).

Model parameterization

Data collected from the above experiments are used to parameterize a population projection model. Five of the parameters in the above model (L_∞, k, γ, μ_0, and α) are estimated as functions of population size (taken as total tank biomass). Each of these density-dependent parameters is represented as a nominal value (at zero tank biomass) minus a power function of tank biomass:

$$f(M) = f_0 - p_1 \cdot M^{p_2}. \tag{7}$$

Parameters of this density-dependent function are fit stepwise for each of the five model parameters. First, the nominal value, f_0, is fit with $p_1 = 0$. Two parameters, f_0 and p_1, are then fit with $p_2 = 1$. Finally all three are fit simultaneously. This stepwise addition of terms proceeds until the reduction in explained variance is no longer significant (F test). Parameters are fit via nonlinear least squares based on the Simplex algorithm (Press et al. 1988).

Total tank biomass is estimated from the measured length–frequency distributions and a fitted relationship between mass and length. This approach is complicated because the length/mass relationships for mature males and females were, themselves, significantly dependent on population biomass (Barlow 1982). Therefore, an iterative approach is used. First, overall length/mass relationships are estimated for males and females (irrespective of tank biomass) based on measured lengths and dry masses. From this, preliminary estimates of tank biomass are made. The density-dependent length/mass relationships are then estimated by making α (Eq. 6) a function of tank biomass (per Eq. 7). Tank biomass is re-estimated. The process of first estimating parameter values and then estimating biomass is repeated until parameter estimates converge.

Somatic growth rates are estimated separately for males and females based on successive measures of distinctly marked fish. Distinctive marks included color patterns in males and caudal pigmentation and "golden" phenotype in some females (Barlow 1982). Data include 1098 measures of paired lengths, typically

TABLE 1. Parameters estimated for the various submodels within the population growth model. The value f_0 represents the nominal value at zero population biomass. Values p_1 and p_2 represent density-dependent modifications to the nominal values as per Eq. 7. Asterisks indicate values that did not add significantly to the goodness of fit. Missing values indicate values for which no attempt was made to fit.

Model	Parameter	f_0	p_1	p_2
Female growth (Eq. 1)	L_∞	37	2.04	2.23
	k	0.12	0.04	*
Male growth (Eq. 1)	L_∞	17	1.03	*
	k	0.24	0.08	*
Brood size (Eq. 3)	γ	1.31×10^{-4}	0.19×10^{-4}	1.97
	ϵ	3.67		
Juvenile survival (Eq. 4)	μ_0	0.73	0.007	6.51
Female mass (Eq. 6)	α	5.09×10^{-6}	1.28×10^{-6}	*
	β	3.19		
Male mass (Eq. 6)	α	3.11×10^{-6}	0.23×10^{-6}	*
	β	3.25		
Juvenile mass (Eq. 6)	α	2.83×10^{-6}	*	*
	β	3.20		

measured from photographs taken 4 wk apart. Parameters L_x and k (Eq. 1) are estimated to minimize the sum of squared residuals between observed and expected lengths. Both parameters are allowed to vary as functions of tank biomass, alternating the stepwise addition of terms (p_1 and p_2) between L_x and k. The nominal value (f_0) for L_x is fixed at 38 mm for females and 17 mm for males; these were the largest individuals measured during the course of the experiment.

The rate of brood production (r in Eq. 2) is estimated as the fraction of mature females that contained distinct embryos (eyespot stage or later) divided by the ontogenetic time required between formation of the eyespot and birth. The fraction of females with embryos was previously estimated by dissecting harvested individuals; this fraction, 0.574, did not vary with population biomass (Barlow 1982). In another series of experiments, the development time between eyespot and birth was measured as 16 d, and it also did not vary with tank biomass (Barlow 1982). The rate of brood production is thus 0.036/d or 0.502/harvest period (27.9 d between broods).

Brood sizes are estimated as a function of female length based on the number of mature eggs and developing embryos seen in dissections of harvested females. Females matured at an average length of 15 mm, and maturation length showed no consistent changes with population biomass (Barlow 1982). The brood size function (Eq. 3) is fit based on brood sizes of 661 mature females (15–38 mm).

Juvenile mortality due to cannibalism could not be measured directly. The juvenile mortality parameter, μ_0, is estimated by minimizing the discrepancies between the observed population growth trajectories and those predicted from the population growth model. The length–frequency distributions were measured in the experimental populations at 4-wk intervals. The predicted length–frequency distribution at the end of each interval is calculated by applying two iterations

of the model to the length–frequency at the beginning of the interval. The parameter, μ_0, is chosen to minimize the squared deviations between the predicted and observed length–frequency distributions. This mortality parameter is allowed to vary as a function of population biomass (per Eq. 7).

Population growth curves

Per capita population growth curves are calculated from the above model by choosing a value for the harvest rate, h, and projecting an arbitrary length–frequency distribution until it reaches a stable population size and length distribution. This process is repeated over a wide range of harvest rates. Per capita growth rate, g, is calculated from harvest rate, h, as

$$g = \frac{1}{(1 - h)} - 1.0. \tag{8}$$

A sustainable harvest rate of 0.25 (25% per harvest period) would thus correspond to a per capita growth rate of 0.33 (33% per harvest period).

RESULTS

Length/mass relationships

Length/mass relationships were strongly density dependent for females, less so for males, and not significantly so for juveniles (Fig. 1). The greater effect in females was largely due to density-dependent fecundity and the mass that developing eggs add to total female mass. The stepwise fitting method indicated that the power parameter (p_2, Eq. 7) is not needed to adequately fit the term α of the length/mass relationship as a function of population biomass for either females or males (Table 1). No density-dependent parameters are needed to adequately fit the length/mass relationship for juveniles. For females, males, and juveniles, mass increases at approximately the 3.2 power of length (β in Table 1).
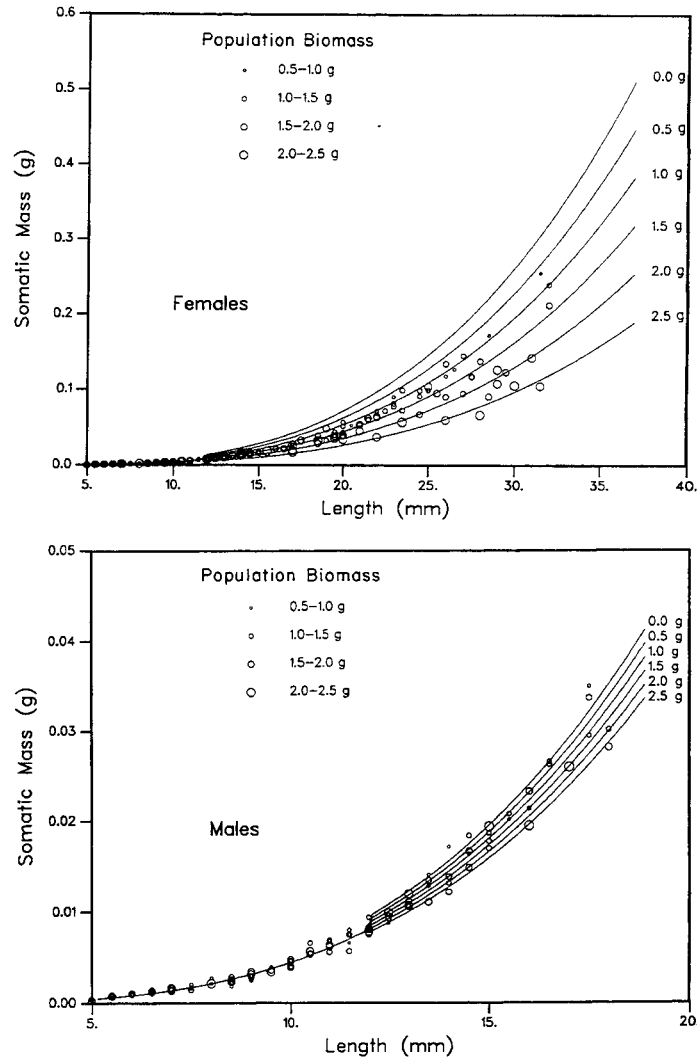
FIG. 1. Somatic mass for females and males expressed as a function of length and population biomass. Illustrated are the observed values for four different ranges of population biomass (O's) and fitted values (——) for six different population sizes (total tank guppy biomasses in grams).

Population biomass

Population biomass is estimated from observed length–frequency distributions and the fitted length/ mass relationships. Trajectories of mean population biomass are shown in Fig. 2. Population biomass appears relatively stable at the higher harvest rates, but at lower harvest rates, the trajectories of population biomass are concave downward. Mean population biomasses for the last 10 harvest periods were 1.81, 1.65, 1.38, 1.29, and 0.96 g (for harvest rates of 5, 10, 15, 20, and 25%, respectively).

Somatic growth rates

Somatic growth rates are strongly density dependent for females and for males (Fig. 3). The stepwise fitting method indicates that the power parameter (p_2, Eq. 7) is not needed to fit the growth parameter, k, but is needed to model changes in asymptotic length as a function of population biomass. The time required to reach sexual maturity in males (≈ 12 mm) varies from 8 wk at a population biomass of 0.5 g to 26 wk at a population biomass of 2.0 g. The time required to reach sexual maturity in females (15 mm) varies from 7 wk
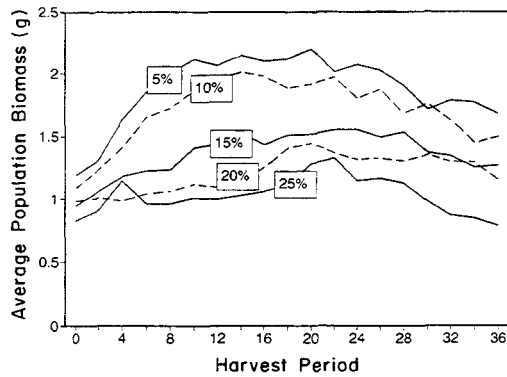
FIG. 2.   Mean population biomass during the course of the experiment for harvest rates of 5, 10, 15, 20, and 25%. Values represent means of three populations with the given harvest rate.

at a population biomass of 0.5 g to 38 wk at a population biomass of 2.0 g.

Brood size

Brood size is also strongly affected by population biomass (Fig. 4). Both density-dependent parameters p_1 and p_2 are required to adequately fit the brood size parameter, γ, as a function of population biomass (Table 1). Brood size increases at approximately the 3.7 power of length, thus increasing in proportion to body mass (which increases at only the 3.2 power of length).

Juvenile survival rates

The nonharvest component of juvenile survival (mostly cannibalism) shows a high degree of density dependence. The exponent of the density response function, p_2, is 6.5 (Table 1), indicating a highly nonlinear response. This is illustrated in Fig. 5, which shows survival rates to be the same at biomasses of 0.0, 0.5, and 1.0 g but decreasing rapidly from biomasses of 1.5–2.5 g.

Population growth rates

Incorporating all aspects of density dependence in the model, the resulting population growth curve is illustrated by the solid line in Fig. 6 (as a function of population biomass). This population growth curve is almost indistinguishable from a logistic growth curve. Per capita growth can be represented as a linear function of population biomass. The only deviation from linearity occurs near zero population biomass. (Little confidence can be put in this extrapolation to zero because parameters were fit based only on population biomasses ranging from 0.5 to 2.5 g.)

Patterns are similar when mean population biomasses for the last 10 harvest periods are plotted as a function of per capita growth rate (Fig. 6). These data

also suggest a linear relationship between biomass and per capita growth. A regression line for the empirical data differs in slope and position from the curve predicted by the model. This could be explained by errors in estimating the 25 parameters that comprise the growth model. It is also likely that the mean biomass for the last 10 harvest periods does not represent the equilibrium biomass for the given harvest rates. Population biomasses appear to have overshot equilibrium for harvest rates of 5, 10, and 15%. Populations may have been in stages of oscillatory approach to equilibrium at the time the experiment ended. Qualitatively, the experiment and model show strikingly similar results.

Alternative population growth curves are calculated based on several scenarios for density dependence (Fig. 7). These include: (1) using a mean fecundity curve without density dependence, (2) using a mean growth rate without density dependence, and (3) using a mean juvenile survival without density dependence.

Discussion

In this simple experimental system, population growth is controlled simultaneously by several density-dependent mechanisms, including reproductive rate, somatic growth rate, and cannibalism. Furthermore, these mechanisms are essentially nonlinear. The best mathematical representations I have found for these mechanisms are nonlinear equations whose parameters are functions (in some cases nonlinear functions) of population biomass. Therefore, it might be viewed as somewhat surprising to find that per capita growth rate is essentially a linear function of population biomass. The combined effect of all the density-compensatory mechanisms is not distinguishable from the simple predictions of the logistic growth curve.

Similar results have been noted before. Three independent studies show that for *Daphnia*, brood size is a concave, nonlinear function of population size (Frank et al. 1957, Smith and Cooper 1982, Kerfoot et al. 1985). In two of these studies, however, per capita population growth is linearly related to population size (Kerfoot et al. 1985). In the third study, per capita growth rate was, like brood size, a concave, nonlinear function of population size (Smith et al. 1988). The lesson is clear. As emphasized by Kerfoot et al. (1985), one must not assume that nonlinearity in a single density-dependent factor will result in nonlinearity in the overall per capita growth curve.

As with the *Daphnia* studies cited above, different studies with guppies have shown different shapes of per capita growth curves. In experiments that were similar to that of Barlow (1982), Silliman and Gutsell (1958) and Silliman (1968) found that per capita growth rates for guppy populations were concave, nonlinear functions of population biomass. Differences in experimental protocol may be responsible for this difference in results. In particular, the harvest scheme of
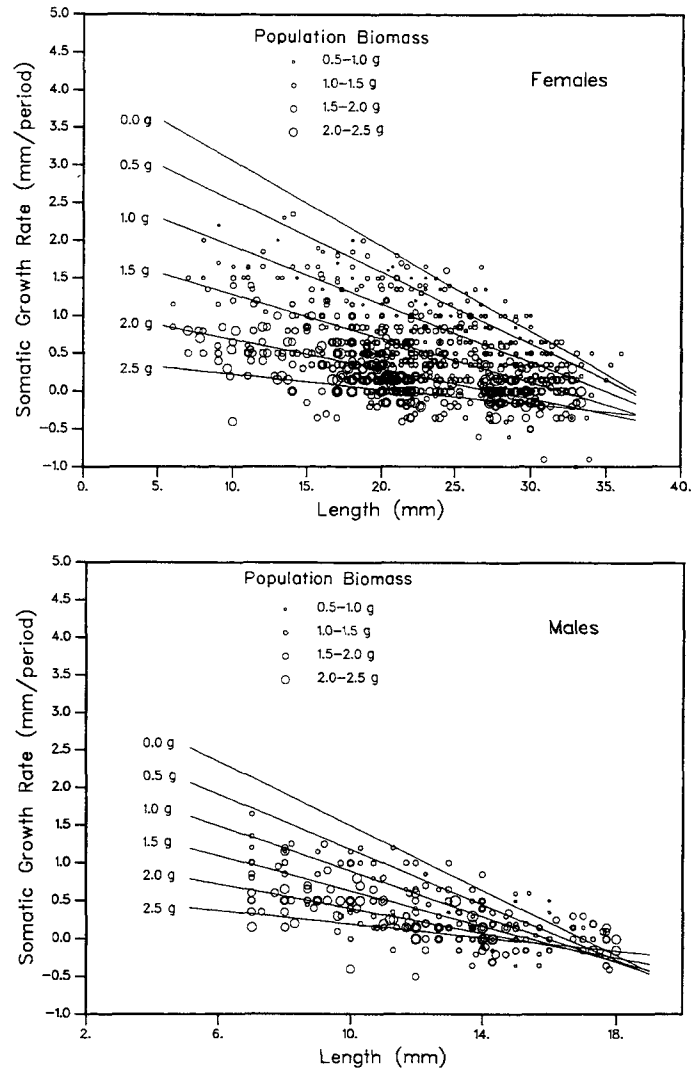
FIG. 3. Somatic growth rate of females and males (expressed in millimetres per 2-wk harvest period) as a function of length and population biomass. Illustrated are the observed values for four different ranges of population biomass (O's) and fitted values (———) for six different population sizes (biomasses in grams).

Silliman and Gutsell (1958) and Silliman (1968) did not include harvest of juveniles. Using a population model, Barlow (1982) showed that this discrepancy in results can be explained solely on the basis of this difference in experimental methods. It is likely that by comparing contradictory experimental results we can learn about how various factors affect density dependence. Instead of quibbling about which experimental protocol is "better" (Smith et al. 1988), we should be asking ourselves whether any generalities can be gleaned by reconciling apparently contradictory results.

In addition to the above lesson, that the sum of many nonlinear effects can be essentially linear, my experiment and model illustrate another important point. All proximate mechanisms of density dependence do not contribute equally to shaping the overall density-dependent response of a population.

As mentioned above, somatic growth, reproductive rates, and cannibalism rates all showed significant changes with population size. By systematically eliminating each of these as density-regulating mechanisms in the model, I examined the role played by each in
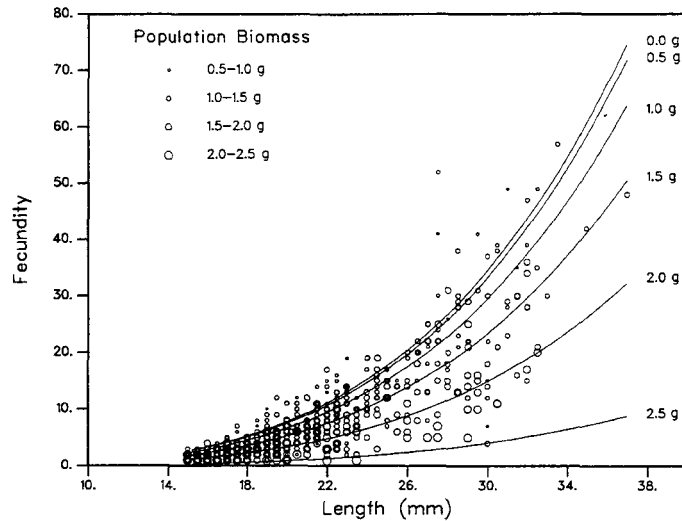
FIG. 4. Brood size (fecundity) expressed as a function of female length and population biomass. Illustrated are the observed values for four different ranges of population biomass (O's) and fitted values (———) for six different population sizes (biomasses in grams).

shaping the overall density-dependent response of the population. Using the full model, per capita growth rate was linearly related to population size. Modifications of the model can be compared to this linear or logistic growth curve.

Density-dependent components of the model were eliminated, one by one, by substituting the mean parameters for the density-dependent parameters given in Table 1. Models without density dependence in reproductive rates and cannibalism rates did not show appreciable change in the overall shape of the per capita

growth curve (Fig. 7). Both could be adequately represented by a logistic growth curve (although there is a slight tendency for the model without density-dependent reproduction to be concave downward). When density dependence in somatic growth rates was eliminated from the model, the population growth curve changed considerably (Fig. 7). In the resulting model, per capita growth rate was essentially constant up to approximately half of carrying capacity, and then decreased rapidly.

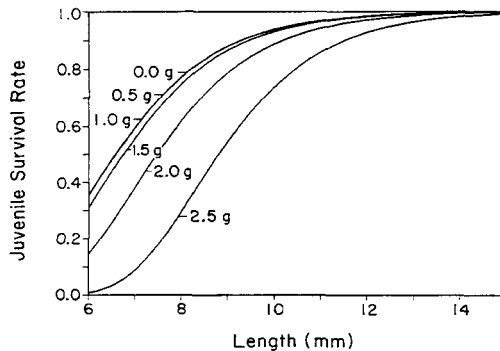The framework for discussing components of density

FIG. 5. Juvenile survival rate (excluding the harvest component of mortality) expressed as a function of length and population biomass. Illustrated are fitted values for six different population sizes (biomasses in grams). Survival rates were not measured directly, rather parameter values were chosen to give the best fit of the population growth model to the observed population trajectories.
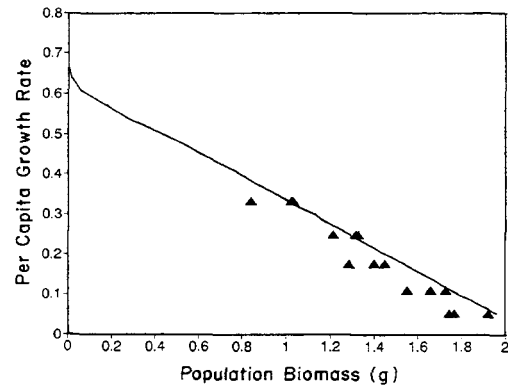

FIG. 6. Equilibrium population biomass and population size as functions of per capita growth rate (as defined by harvest rate) for the experiment, ▲, and for the model (———). Equilibrium population biomasses for the experiment are estimated as the mean values for the last 10 harvest periods.
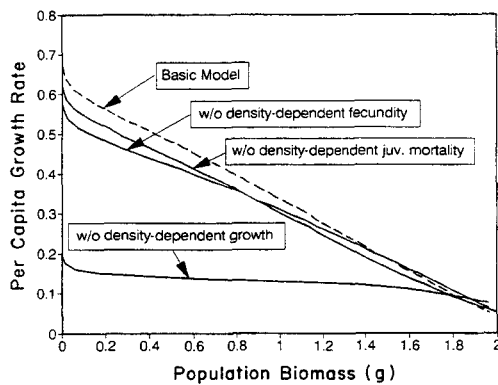
FIG. 7. Equilibrium population biomass as a function of per capita growth rate (as defined by harvest rate) for the basic model and for three special cases of the model: (1) excluding (w/o = without) density dependence in brood size, (2) excluding density dependence in growth rates, and (3) excluding density dependence in juvenile survival rates.

dependence has typically centered on birth rates and death rates (b and d, Kerfoot et al. 1985). Somatic growth rates affect overall b and d, even though length-specific rates, $b(L)$ and $d(L)$, are not affected by growth rates. By growing slower, juveniles remain at a vulnerable size for a longer period, thus increasing their risk of mortality by cannibalism. Similarly, slow growth reduces effective fecundity by making females smaller at any given age. As was seen in Fig. 7, density dependence could be eliminated in length-specific fecundity or in juvenile survival rates without appreciably changing the shape of the density-dependent response. At least with species that show indeterminate growth, such as fish, somatic growth rates are likely to be very important in shaping per capita growth curves.

The importance of density dependence in somatic growth rates has been noted previously by several researchers working on fish and amphibian populations. Wilbur (1977) showed that increasing tadpole density did not affect larval toad survival rates but greatly affected the probability of surviving from egg to metamorphosis via its effect on somatic growth rates. In a near natural pond, Werner et al. (1983) showed that the somatic growth rate of bluegill fish (*Lepomis macrochirus*) is affected by predatory fish density. The latter work not only indicates the importance of plasticity in fish growth rates outside the laboratory, but also emphasizes the trade-off between optimal foraging (and high growth rate) and the potential for predatory mortality. Similar trade-offs may have existed between growth rate and cannibalism for juvenile guppies in my experimental system.

As a final note, I want to emphasize an often ignored point regarding density dependence in population growth. Numerical abundance and biomass have both been used as measures of population size in population

growth models. Fisheries data are typically in units of biomass (such as tons of fish landed); hence, most fisheries population models are expressed in terms of biomass (Schaefer 1954, Ricker 1958, Pella and Tomlinson 1969, etc.). To terrestrial ecologists, population size is typically taken to mean numerical abundance (Gilpin and Ayala 1973, May 1974, Goh 1977, etc.). In fact, the same models are used by both groups whether referring to numbers or biomass (Pomerantz et al. 1980). To further complicate matters, those who have made predictions regarding the expected shape of population growth curves have failed to specify whether their predictions apply only to numbers, to biomass, or to both (Gilpin and Ayala 1973, Gilpin et al. 1976, May et al. 1979, Fowler 1981).

In fact, however, the units of measure do matter. Although a full explanation would require another paper, it is worth noting that the per capita growth curve from the experiment described here looks very different when expressed as a function of population number rather than biomass (Barlow 1982). The reason is that the size-frequency distributions are not the same at different population growth rates. Because mass is nonlinearly related to length, total population number will not be linearly related to population biomass *unless* the size-frequency distribution does not change. If the size-frequency distribution does change with different population growth rates, per capita growth rate cannot be linearly related to both population number and biomass.

LITERATURE CITED

Barlow, J. 1982. Density compensation and the dynamics of growth in experimental fish populations. Pages 97–177 *in* Methods and applications in estimating mortality and other vital rates. Dissertation. University of California, San Diego, California, USA.

Breder, C. M., and C. W. Coates. 1932. A preliminary study of population stability and sex ratio of *Lebistes*. Copeia 1932:145–155.

Frank, P. W. 1957. Coaction in laboratory populations of two species of *Daphnia*. Ecology 38:510–519.

Fowler, C. W. 1981. Density dependence as related to life history strategy. Ecology 62:602–610.

———. 1988. Population dynamics as related to rate of increase per generation. Evolutionary Ecology 2:197–204.

Gill, D. E. 1978. On selection at high population density. Ecology 59:1289–1291.

Gilpin, M. E., and F. J. Ayala. 1973. Global models of growth and competition. Proceedings of the National Academy of Sciences (USA) 70:3590–3593.

Gilpin, M. E., T. J. Case, and F. J. Ayala. 1976. Θ-Selection. Mathematical Biosciences 32:131–139.

Goh, B. S. 1977. Global stability in many-species systems. American Naturalist 111:135–143.

Goodman, D. 1980. The maximum yield problem: distortion in the yield curve due to age structure. Theoretical Population Biology 18:160–174.

Kerfoot, W. C., W. R. DeMott, and C. Levitan. 1985. Nonlinearities in competitive interactions: component variables or system response. Ecology 66:959–965.

Kingsland, S. E. 1985. Modeling nature: episodes in the history of population ecology. University of Chicago Press, Chicago, Illinois, USA.

Laakso, M. 1959. The influence of population density and harvesting techniques on growth of the common guppy *Lebistes reticulatus.* Dissertation. University of Minnesota, Minneapolis, Minnesota, USA.

May, R. M. 1974. Biological populations with nonoverlapping generations: stable points, stable cycles, and chaos. Science 186:645–647.

May, R. M., J. R. Beddington, C. W. Clark, S. J. Holt, and R. M. Laws. 1979. Management of multispecies fisheries. Science 205:267–277.

Pella, J. J., and P. K. Tomlinson. 1969. A generalized stock production model. Bulletin of the Inter-American Tropical Tuna Commission 13:420–496.

Pomerantz, M. J., W. R. Thomas, and M. E. Gilpin. 1980. Asymmetries in population growth regulated by intraspecific competition: empirical studies and model tests. Oecologia (Berlin) 47:311–322.

Press, W. H., B. P. Flannery, S. A. Teukolsky, and W. T. Vetterling. 1988. Numerical recipes: the art of scientific computing. Cambridge University Press, Cambridge, England.

Ricker, W. E. 1958. Handbook of computations for biolog-ical statistics of fish populations. Bulletin of the Fisheries Research Board of Canada 119.

Schaefer, M. B. 1954. Some aspects of the dynamics of populations important to the management of the commercial marine fisheries. Bulletin of the Inter-American Tropical Tuna Commission 1:27–56.

Shoemaker, H. H. 1944. A laboratory study of fish populations. Transactions of the American Fisheries Society 74: 350–359.

Silliman, R. P. 1968. Interaction of food level and exploitation in experimental fish populations. United States National Marine Fisheries Service Fishery Bulletin 66:425–439.

Silliman, R. P., and J. S. Gutsell. 1958. Experimental exploitation of fish populations. United States National Marine Fisheries Service Fishery Bulletin 58:215–252.

Smith, D. W., and S. D. Cooper. 1982. Competition among cladocera. Ecology 63:1004–1015.

Smith, D. W., S. D. Cooper, and O. Sarnelle. 1988. Curvilinear density dependence and the design of field experiments on zooplankton competition. Ecology 69:868–870.

Smith, F. E. 1963. Population dynamics in *Daphnia magna* and a new model for population growth. Ecology 44:651–663.

Smith, T. D. 1983. Changes in size of three dolphin (*Stenella* spp.) populations in the eastern tropical Pacific. United States National Marine Fisheries Service Fishery Bulletin 81:1–13.

Werner, E. E., J. F. Gilliam, D. J. Hall, and G. G. Mittelbach. 1983. An experimental test of the effects of predation risk on habitat use in fish. Ecology 64:1540–1548.

Wilbur, H. M. 1977. Density-dependent aspects of growth and metamorphosis in *Bufo americanus.* Ecology 58:196–200.